Available online at www.sciencedirect.com
SCIENCE DIRECT
Composites: Part B 36 (2005) 183–187
composites Part B: engineering
www.elsevier.com/locate/compositesb

Processing, structure, and properties of carbon nano fiber filled PBZT composite fiber

Tetsuya Uchida[c], Thuy Dang[b], B.G. Min[d], Xiefei Zhang[a], Satish Kumar[a,*]

[a]School of Polymer, Textile and Fiber Engineering, Georgia Institute of Technology, Atlanta, Georgia 30332-0295, USA
[b]Polymer Branch, Air Force Research Laboratory, WPAFB OH 45433, USA
[c]Faculty of Engineering, Okayama University, Okayama 700-8530, Japan
[d]School of Advanced Materials and System Engineering, Kumoh Institute of Technology, Kumi 730-731, South Korea

Received 1 March 2004; accepted 19 April 2004
Available online 4 August 2004

Abstract

The poly(*p*-phenylene benzobisthiazole) (PBZT)/carbon nano fiber (CNF) composite was prepared by in situ polymerization in polyphosphoric acid (PPA), and fibers spun by dry-jet wet spinning. The liquid crystalline PBZT/CNF dope in PPA exhibited excellent spinnability. The PBZT/CNF weight ratio was 90/10. The transmission electron microscope images show isolated and well oriented CNFs with no aggregation. CNF graphite layer stacking in the composite fiber have been observed using high resolution transmission electron microscopy, and showed that graphitic structure of CNFs was not damaged during polymerization in PPA and subsequent fiber spinning and drawing. High resolution transmission electron microscopy also shows that there is no debonding between CNF and the PBZT matrix. Tensile and compressive properties of the composite fibers have been determined and discussed.

Keywords: Carbon nano fiber

1. Introduction

Vapor grown carbon nano fibers (CNFs) and carbon nanotubes (CNTs) are drawing significant attention worldwide for their potential applications in nano-scale polymer reinforcement. The primary interest of this paper is vapor grown CNF, which is synthesized from the pyrolysis of hydrocarbons or carbon monoxide in the gaseous state, in the presence of a catalyst [1–3]. Vapor grown CNFs distinguish themselves from other types of nano fibers, such as polyacrylonitrile- or mesophase pitch-based carbon fibers, in its method of production, physical properties, and structure.

CNF reinforced composites have been processed using variety of matrices. These include commodity polymers, including polypropylene [4–7], polycarbonate [8,9], nylon [10], poly(methyl methacrylate) [11,12], poly(ether ether ketone) [13], polyamide [14], PET [15], and epoxy [16]. These studies reported varying degree of success in achieving CNF dispersion and orientation as well as in improving mechanical and thermal properties. In these studies, with the exception of epoxy, CNF has been blended in the polymer matrix during melt processing.

In the current study, poly(*p*-phenylene benzobisthiazole) (PBZT) has been polymerized in poly (phosphoric acid) (PPA) in the presence of CNFs, and the PBZT/CNF composite fibers have been spun from the resulting liquid crystalline dope using dry jet wet spinning. The PBZT is a rigid-rod polymer and the PBZT and PBO fibers are among the most stiff and thermally stable polymer [17–20]. Tensile properties of the composite fiber have been studied and its structure has been elucidated using high resolution transmission electron microscopy. A morphological study of the CNFs will be published separately [21].

* Corresponding author.
E-mail address: satish.kumar@ptfe.gatech.edu (S. Kumar).

1359-8368/$ - see front matter © 2004 Elsevier Ltd. All rights reserved.
doi:10.1016/j.compositesb.2004.04.015

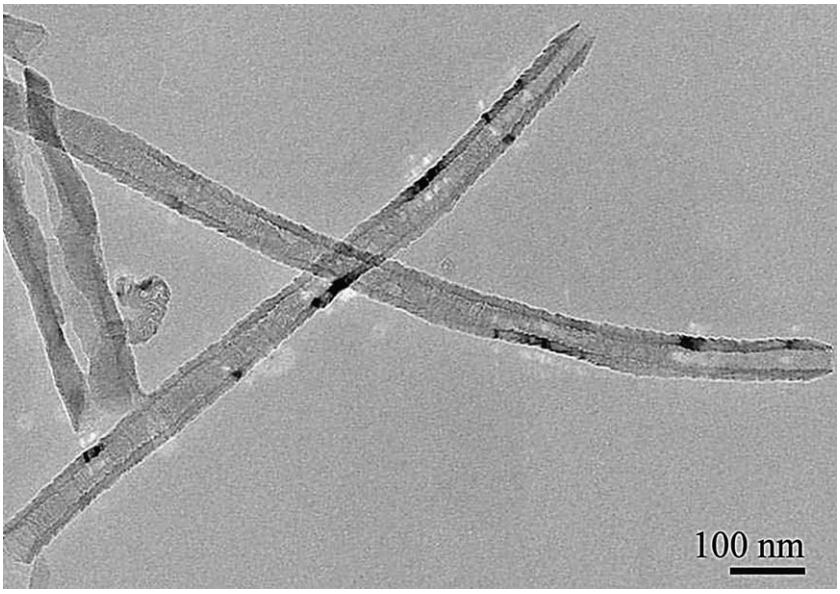

Fig. 1. Transmission electron micrograph of the carbon nano fiber.

2. Experimental

Vapor grown CNF (AS PR-24-HT), synthesized using metal catalyst was obtained from Applied Sciences Inc., Cedarville, Ohio. Heat treatment of the nano fiber was performed at 3000 °C in inert environment. Thermogravimetric analysis (TGA) results show that the metallic impurity in this sample is less than 5wt%. The average CNF outer diameter is ~80 nm and the inner diameter of the hollow core is ~30 nm (Fig. 1). The length of the as received nano fiber was in the 1–30 μm range, with the number average length of ~2 μm. CNF length after in situ polymerization was not determined, however due to continuous high shear mixing for over 24 h during polymerization, CNF length is likely to decrease. Graphite planes in these nano fibers are oriented at an angle of 15° with respect to the nano fiber axis. As a result, the lower bound limit of the CNF tensile modulus along its axis is only 50 GPa, while the tensile modulus of the graphite along the basal planes is 1060 GPa. CNF morphological structural details and modulus calculations are reported elsewhere [21].

The PBZT/CNF composite dope was prepared by in situ polycondensation of bis(aminothiophenol) and terepthalic acid in the presence of CNFs. The in situ polycondensation is carried out in PPA to give solids (PBZT/CNF) concentration of 10% by weight, which forms an anisotropic reaction mixture. Intrinsic viscosity of the PBZT extracted from the composite dope was 28 dl/g measured in methane sulfonic acid at 30 °C. This polymerization method is similar to the one used for synthesizing poly (*p*-phenylene benzobisoxazole) (PBO)/single wall carbon nanotube (SWNT) composite dope in PPA [22].

PBZT/CNF fibers were dry-jet wet spun using a piston driven spinning system manufactured by Bradford University Research Ltd. For fiber spinning, polymer dope was heated to 100 °C. In the spinning of PBO, PBZT, and PBO/SWNT a filter has generally been used in the spin line. However, PBZT/CNF study was carried out without filter. Spun fibers were continuously washed in water for one week, vacuum dried at 80 °C for 12 h and, subsequently, heat-treated in nitrogen under tension for 2 min at 400 °C.

For tensile testing, fibers were mounted on cardboard tabs. Testing was performed on an Instron universal tensile tester (model 5567) using 2.54 cm gage length at a strain rate of 2%/min. About 20 samples were tested in each case. Fiber diameters were measured using laser diffraction. Stress–strain curves for both the PBZT and PBZT/CNF were fairly linear and similar to the once previously reported for PBO and PBO/SWNT fibers [22]. Thin specimens for the transmission electron microscopy were prepared using detachment replication method [23,24]. Bright field and dark field images as well as selected area electron diffraction patterns were recorded on Kodak Microscope Film (SO163) using a high resolution electron microscope (JEM 4000EX) operated at 400 kV.

3. Results and discussion

PBZT/CNF dope in PPA exhibited excellent fiber spinnability. From a 250 μm diameter single hole spinneret,

Table 1
Properties of PBZT and PBZT/CNF composite fibers

Sample	Tensile strength (GPa)	Tensile modulus (GPa)	Elongation to break (%)
PBZT [25]	2.8	224	1.3
PBZT + 10 wt% Carbon nano fiber	1.6	150	1.1

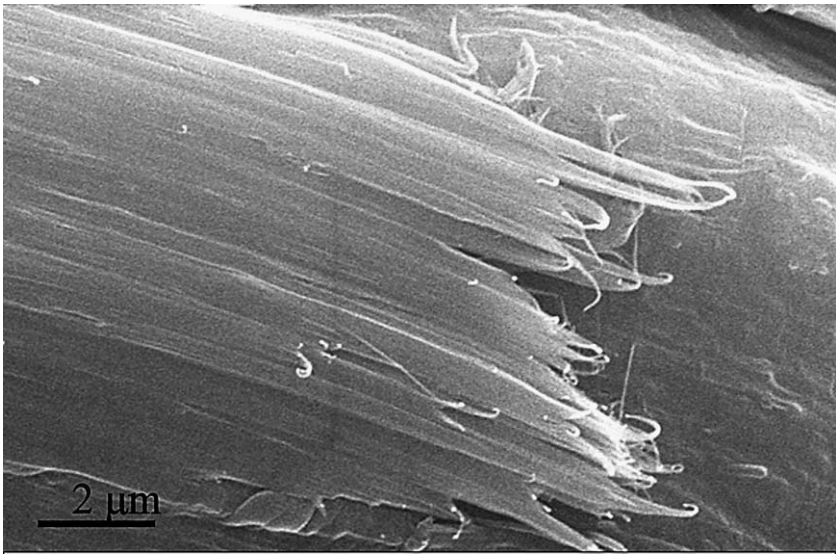

Fig. 2. Scanning electron micrograph of the tensile fracture surface of the PBZT/CNF composite fiber.

fibers of 15 μm diameters could be drawn. Good fiber processability of the PBZT/CNF composite suggests that during the in situ polymerization, CNFs were well dispersed in the PBZT solution, a conclusion confirmed by transmission electron microscopy.

Tensile properties of the composite fiber are lower than those of the control PBZT fiber (Table 1). Decrease in the composite fiber modulus can be attributed to the relatively low intrinsic modulus of the CNF [21]. Previous work on PBO/SWNT composite [22] showed that the tensile strength of the composite fiber was higher than that of the control PBO fiber when ultrahigh purity SWNTs (catalyst metal impurity ~1 wt%) were used. Higher levels of catalytic impurity in the CNFs used in this study may at least in part be responsible for low tensile strength of the PBZT/CNF composite fibers. In addition, interaction between CNF surface and PBZT molecule and between SWNT and PBO molecule may be different, which may result in lower tensile strength in PBZT/CNF composite fiber. Differences in SWNT and CNF length will also affect the composite fiber tensile strength. The compressive strength of the PBZT/CNF composite fiber measured from recoil test [26] is ~400 MPa, while the compressive strength values for PBZT measured from recoil test are generally in the 200–300 MPa range. A moderate increase in compressive strength with the presence of CNFs was also observed in PET/CNF composite fiber [15]. Polymeric fibers in compression fail due to kinking. It is expected that the presence of CNFs arrests the propagation of the kink, delaying the compression failure.

Scanning electron micrograph of the composite fiber (Fig. 2) showed fibrillar structure, a feature also observed for the control PBZT fiber. Because of this fibrillar structure, the CNF in the composite fiber could not be observed clearly, as it could not be distinguished from the PBZT fibrils. Therefore, to study the structural features of the CNFs in the PBZT/CNF composite, transmission electron microscopy was employed. Transmission electron micrograph of the PBZT/CNF composite fiber is shown in Fig. 3. In this image, individual CNFs are clearly observed in the PBZT matrix. Extensive transmission electron microscope (TEM) studies showed no aggregation of CNFs in the PBZT/CNF composite fiber. Though the quantitative analysis of CNF length in the PBZT/CNF

Fig. 3. Transmission electron micrograph of the PBZT/CNF composite fiber (bright field image).

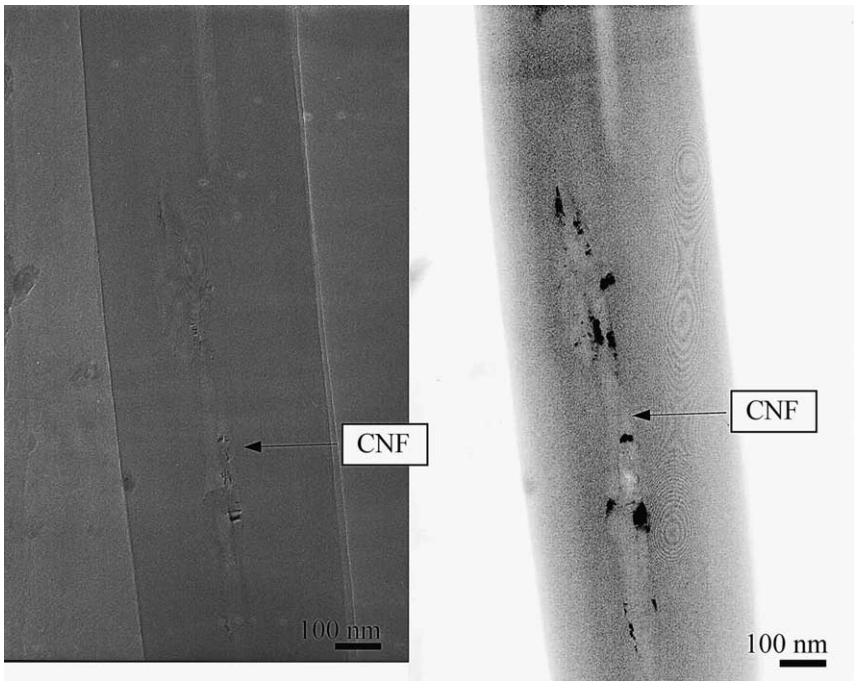

Fig. 4. Transmission electron micrographs of the PBZT/CNF composite fiber. Bright field image on the left and dark field image on the right.

composite fiber was not done, most CNFs appeared to be of the order of a few micrometers in length. These observations suggest that CNF length did not decrease drastically [21], during in situ polymerization of PBZT in PPA. Transmission electron microscopy observations also suggest that CNFs are well aligned along the composite fiber axis. Well aligned and isolated CNFs observed in the composite fiber suggests that during the in situ polymerization of PBZT, the CNF are well dispersed in the dope, and CNF alignment occurs during fiber spinning and to some extent during heat treatment under tension. However, curvature in the CNF fiber can still be observed in the transmission electron microscopy image. The presence of such a curvature would also reduce mechanical properties, particularly tensile modulus. Dark field image observed from (002) graphite electron diffraction peak in CNF also show the presence of CNFs in the composite fiber (Fig. 4).

High resolution transmission electron micrograph of the PBZT/CNF composite fiber (Fig. 5) clearly shows the stacking phenomenon of the graphite layer in the CNF. Fig. 5 shows that in spite of harsh polymerization conditions

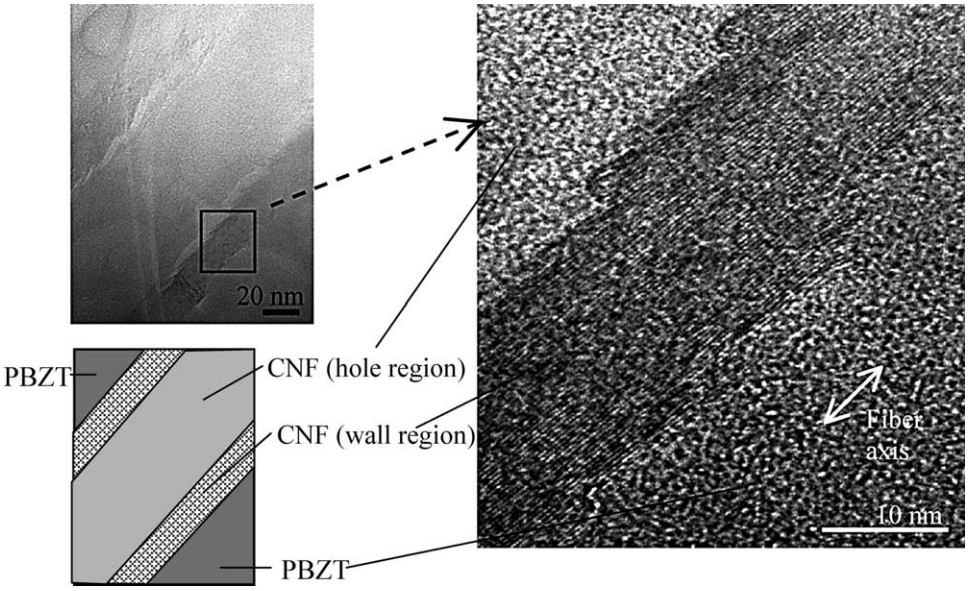

Fig. 5. High resolution transmission electron micrographs of the PBZT/CNF composite fiber.

(strong acid, high viscosity, and mixing/stirring for over 24 h) and subsequent fiber processing (drawing during fiber spinning and heat treatment), the graphitic order in CNFs has not been damaged. Close observation also reveal relatively smooth interface between the CNF and PBZT without any voids. To be able to discern interface differences in PBO/SWNT and in PBZT/CNF would require more extensive high resolution transmission electron microscopy study on these system than has been carried out to-date.

4. Conclusions

This study demonstrates that CNFs can be blended in rigid-rod polymers during in situ polymerization. These liquid crystalline dispersions exhibit excellent fiber processability and CNT alignment along the fiber axis. CNFs are not damaged during harsh polymerization and fiber processing conditions. High resolution transmission electron microscopy also show that there are no voids at the boundary of CNF and PBZT suggesting good interaction between the two components.

Acknowledgements

This work was supported by Air Force Office of Scientific Research (grant # F49620-00-1-0147) and National Science Foundation.

References

[1] Tibbetts GG, Devour MG. US Pat. 4,565,684; January 21, 1986.
[2] Lake ML, Ting JM. Vapor grown carbon fiber composites. In: Burchell TD, editor. Carbon Materials for Advanced Technologies. Oxford, UK: Pergamon Press; 1999, p. 139–67.
[3] De Jong KP, Geus JW. Carbon nanofibers: catalytic synthesis and applications. Catal Rev-Sci Eng 2000;42(4):481–510.
[4] Tibbetts GG, McHugh JJ. Mechanical properties of vapor-grown carbon fiber composites with thermoplastic matrices. J Mater Res 1999;14(7):2871–80.
[5] Lozano K, Barrera EV. Nanofiber-reinforced thermoplastic composites. 1. Thermoanalytical and mechanical analyses. J Appl Polym Sci 2000;79(1):125–33.
[6] Kuriger RJ, Alam MK, Anderson DP, Jacobsen RL. Processing and characterization of aligned vapor grown carbon fiber reinforced polypropylene. Composites Part A 2002;33:53–62.
[7] Kumar S, Doshi H, Srinivasarao M, Park JO, Schiraldi DA. Fibers from polypropylene/nano carbon fiber composites. Polymer 2002;43:1701–3.
[8] Caldeira G, Maia JM, Carneiro OS, Covas JA, Bernardo CA. Production and characterization of innovative carbon fiber-polycarbonate composites. Polym Compos 1998;19(2):147–51.
[9] Carneiro OS, Maia JM. Rheological behavior of (short) carbon fiber/thermoplastic composites. Part II: the influence of matrix type. Polym Compos 2000;21(6):970–7.
[10] Pogue RT, Ye J, Klosterman DA, Glass AS, Chartoff RP. Evaluating fiber–matrix interaction in polymer–matrix composites by inverse gas chromatography. Composites Part A 1998;29:1273–81.
[11] Cooper CA, Ravich D, Lips D, Mayer J, Wagner HD. Distribution and alignment of carbon nanotubes and nanofibrils in a polymer matrix. Compos Sci Technol 2002;62:1105–12.
[12] Zeng J, Saltysiak B, Johnson WS, Schiraldi DA, Kumar S. Processing and properties of poly(methyl methacrylate)/carbon nano fiber composite. Composites Part B 2004;35(2):173–8.
[13] Sandler J, Windle AH, Werner P, Altstadt V, Es MV, Shaffer MSP. Carbon-nanofiber-reinforced poly(ether ether ketone) fibers. J Mater Sci 2003;38(10):2135–41.
[14] Cadek M, Le Foulgoc B, Coleman JN, Barron V, Sandler J, Shaffer MSP, Fonseca A, van Es M, Schulte K, Blau WJ. Mechanical and thermal properties of CNT and CNF reinforced polymer composites. AIP Conf Proc: Struct Electron Prop Mol Nanostruct 2002;633:562–5.
[15] Ma H, Zeng J, Realff ML, Kumar S, Schiraldi DA. Processing, structure, and properties of fibers from polyester/carbon nanofiber composites. Compos Sci Technol 2003;63:1617–28.
[16] Patton RD, Pittman CU, Wang L, Hill JR. Vapor grown carbon fiber composites with epoxy and poly(phenylene sulfide) matrices. Composites: Part A 1999;30:1081–91.
[17] Adams WW, Eby RK, McLemore DE, editors. The materials science and engineering of rigid-rod polymers. Materials Research Society Symposium Proceedings, Pittsburgh, PA, 1989, p. 134.
[18] Kumar S. In: Lee SM, editor. Ordered polymeric fibers. International Encyclopedia of Composites, vol. 4. New York: VCH; 1991, p. 51–74.
[19] Kuroki T, Tanaka Y, Hokudoh T, Yabuki K. Heat resistance properties of poly(*p*-phenylene-2,6-benzobisoxazole) fiber. J Appl Polym Sci 1997;65:1031–6.
[20] Hu X, Jenkins SE, Min BG, Polk MB, Kumar S. Rigid-rod polymers: synthesis, processing, simulation, structure, and properties. Macromol Mater Eng 2003;288(11):823–43.
[21] Uchida T, Anderson DP. Morphology and Modulus of Vapor Grown Carbon Nano Fibers. To be published.
[22] Kumar S, Dang TD, Arnold FE, Bhattacharyya AR, Min BG, Zhang X, Vaia RA, Park C, Adams WW, Hauge RH, Smalley RE, Ramesh S, Willis PA, Kumar S. Synthesis, structure, and properties of PBO/SWNT composites. Macromolecules 2002;35:9039–43.
[23] Shimamura K, Minter JR, Thomas EL. Lattice imaging of high modulus poly (*p*-phenylene benzobisthiazole) fibers. J Matter Sci Lett 1983;18:54–8.
[24] Adams WW, Kumar S, Martin DC, Shimamura K. Lattice imaging of poly(*p*-phenylene benzobisoxazole) (PBO) fiber. Polym Commun 1989;30(9):285–7.
[25] Mehta VR, Kumar S. Structure, morphology, and properties of PBZT and methyl pendant PBZT fibers. J Appl Polym Sci 1999;73:305–14.
[26] Kozey VV, Jiang H, Mehta VR, Kumar S. Compression behavior of materials: Part II—high performance fibers. J Mater Res 1995;10:1044–61.